HHS Public Access

Author manuscript

Int J Cancer. Author manuscript; available in PMC 2017 February 15.

Published in final edited form as:

Int J Cancer. 2016 February 15; 138(4): 1013–1023. doi:10.1002/ijc.29831.

A Potent Immunotoxin Targeting Fibroblast Activation Protein for Treatment of Breast Cancer in Mice

Jinxu Fang[a,1], **Liang Xiao**[a,1], **Kye-Il Joo**[a], **Yarong Liu**[a], **Chupei Zhang**[a], **Shuanglong Liu**[b], **Peter S. Conti**[b], **Zibo Li**[b], and **Pin Wang**[a,c,d,*]

[a]Mork Family Department of Chemical Engineering and Materials Science, University of Southern California, Los Angeles, CA 90089

[b]Molecular Imaging Center, Department of Radiology, University of Southern California, Los Angeles, CA 90033

[c]Department of Biomedical Engineering, University of Southern California, Los Angeles, CA 90089

[d]Department of Pharmacology and Pharmaceutical Sciences, University of Southern California, Los Angeles, CA 90089

Abstract

Fibroblast activation protein (FAP) is highly expressed in the tumor-associated fibroblasts (TAFs) of most human epithelial cancers. FAP plays a critical role in tumorigenesis and cancer progression, which makes it a promising target for novel anticancer therapy. However, mere abrogation of FAP enzymatic activity by small molecules is not very effective in inhibiting tumor growth. In this study, we have evaluated a novel immune-based approach to specifically deplete FAP-expressing TAFs in a mouse 4T1 metastatic breast cancer model. Depletion of FAP-positive stromal cells by FAP-targeting immunotoxin αFAP-PE38 altered levels of various growth factors, cytokines, chemokines and matrix metalloproteinases, decreased the recruitment of tumor infiltrating immune cells in the tumor microenvironment and suppressed tumor growth. In addition, combined treatment with αFAP-PE38 and paclitaxel potently inhibited tumor growth *in vivo*. Our findings highlight the potential use of immunotoxin αFAP-PE38 to deplete FAP-expressing TAFs and thus provide a rationale for the use of this immunotoxin in cancer therapy.

Keywords

immunotoxin; fibroblast activation protein; tumor-associated fibroblast; breast cancer; tumor microenvironment; positron emission tomography (PET)

*Corresponding author: Mork Family Department of Chemical Engineering and Materials Science, University of Southern California, 3710 McClintock Ave., RTH509, Los Angeles, CA 90089, Phone: (213)-740-0780, Fax: (213)-740-8053, pinwang@usc.edu.

[1]These authors contributed equally to this work

Disclosure of Potential Conflicts of Interest

No potential conflicts of interest were disclosed.

Introduction

Tumorigenesis is a complex multistep process involving not only genetic and epigenetic alterations in tumor cells, but also other cells in the dysregulated microenvironment surrounding the tumor, e.g., immune and inflammatory cells, endothelial cells and tumor-associated fibroblasts (TAFs), collectively termed herein as stromal cells. Stromal cells communicate with tumor cells, as well as inflammatory and immune cells, directly via cell interaction and indirectly via paracrine/exocrine signaling, protease activity and modulation of extracellular matrix (ECM) properties that alter cell-cell tension[1]. Such complex crosstalk results in a tumor microenvironment that supports tumorigenesis, angiogenesis and metastasis[1, 2].

TAFs are primarily responsible for the synthesis, deposition, and remodeling of the ECM, as well as the production of growth factors, cytokines and chemokines, promoting tumor growth and metastasis[3–5]. The degradation of extracellular matrix depends on matrix metalloproteinases (MMPs)[6]. MMP-2 and MMP-9 are expressed in tumor-derived fibroblasts[7], and their expression is associated with the invasiveness of many human cancers[8]. They play an important role in tumor angiogenesis by regulating the release of vascular endothelial growth factor (VEGF), the most potent inducer of tumor angiogenesis[6]. Primary TAFs extracted from breast carcinoma patients displayed increased expression of SDF-1 and TGF-β mRNA and enhanced TGF-β bioactivity[9]. Autocrine TGF-β and SDF-1 signaling drives the differentiation of tumor-promoting TAFs during tumor progression[9]. TAFs also express tumor necrosis factor-alpha (TNF-α), which can induce acute, hypoxic death of both cancer and stromal cells[10], and the chemokine monocyte chemotactic protein-1 (MCP-1), which critically mediates the recruitment of macrophage cells[11]. Given the essential roles of TAFs in tumor progression and metastasis, they have recently emerged as new promising therapeutic targets[12–14].

Fibroblast activation protein (FAP) is expressed remarkably in TAFs in most human epithelial cancers as well as in some soft tissue and bone sarcomas[12]. It was also detected in the stroma of human prostate cancer specimens[15] and in the fibroblasts or pericytes in areas of tumor angiogenesis[16]. FAP has emerged as a key regulator in cancer physiology with multiple biological functions, such as cell motility, cell adhesion, cell invasion and angiogenesis[17–19]. Expression of either catalytically active or inactive FAP enhanced the production of MMP-9 and invasive behavior of cells[20, 21]. In addition, FAP-expressing stromal cells have been shown to suppress antitumor immunity[10], adding another layer of complexity in FAP-mediated tumor growth.

The dipeptidyl-peptidase activity of FAP contributes to tumor progression, as suggested by the finding that abrogation of FAP enzymatic activity attenuates the growth of HT-29 colon carcinoma cells[22, 23]. Most FAP-based therapeutic approaches have focused on the development of small-molecule inhibitors of enzymatic activity[16, 24–26]. However, inhibition of FAP enzymatic activity by small molecules has had little success to date in clinical trials[17]. This could be attributed to the cyclization of these small molecules, rendering them ineffective at the tumor site, or the non-enzymatic functions of FAP in tumor progression,

based on recent evidence showing that a catalytically inactive mutant of FAP promotes tumor growth and invasion of breast cancer cells through non-enzymatic functions[20].

More recently, rationally designed immunotoxins that target cell-surface proteins have emerged as a promising approach for cancer treatment[27, 28]. The most commonly used immunotoxins are based on diphtheria toxin (DT) and Pseudomonas exotoxin (PE), both of which prevent protein synthesis by inactivating EF-2 through ADP ribosylation. Immunotoxins have been proven to effectively inhibit tumor growth. For example, anti-Fc receptor-like 1 (FCRL1) immunotoxin E9(Fv)-PE38 displayed remarkably selective cytotoxicity on FCRL1-positive malignancies. Immunotoxin IL4-PE potently inhibited growth of human glioblastoma tumors[29]. Furthermore, many different immunotoxins have already been clinically evaluated[30]. Among them, DT-IL2 has been approved by the Federal Drug Administration (FDA) for treatment of cutaneous T-cell lymphoma (CTCL)[27].

In this study, we constructed the novel immunotoxin αFAP-PE38 designed to target FAP-expressing fibroblasts within the tumor stroma and tested its efficacy in suppressing tumor growth in a mouse 4T1 metastatic breast cancer model. In addition, we also investigated the molecular mechanism underlying its inhibition of tumor growth. Finally, we explored the possible combination therapy of αFAP-PE38 and paclitaxel in the same mouse model.

Materials and Methods

Mice, cell line construction and cell culture

Female BALB/c mice were purchased from Harlan Laboratories and housed in the animal facility in accordance with institute regulations. All animal experiments and protocols were performed according to the guidelines set by the NIH and the University of Southern California on the Care and Use of Animals. Murine 4T1 mammary carcinoma cell line was purchased from ATCC. The 293T–hFAP and 293T–mFAP cell lines were generated by stable transduction of 293T cells with lentivirus pseudotyped with vesicular stomatitis virus glycoprotein, as described previously[31]. Both cell lines were cultured in DMEM supplemented with 10% FBS.

Plasmid construction and protein purification

The sequence encoding the truncated Pseudomonas exotoxin A (PE38), and a reported sequence of species-crossreactive FAP-specific scFv (MO36)[32] fused with PE38 were cloned into the pET-28a(+) vector separately. The plasmids were transformed to *Escherichia coli* BL21 (DE3; Invitrogen) and the bacteria were grown in luria broth media containing 100 μg/ml of kanamycin at 37°C until OD_{600} reached 0.6, followed by the addition of isopropyl-β-D-1-thiogalactopyranoside (IPTG, 1 mM) for 4 hours. Cells were then harvested and the recombinant fusion protein was isolated from inclusion bodies by washing with 2M urea buffer and dissolving in 8M urea. After renaturation by dialysis in gradient urea buffer, the recombinant fusion protein was subject to Ni^{2+}-IDA column for His-tag-based purification.

Dye labeling of αFAP-PE38 and immunofluorescence imaging

To label αFAP-PE38 with organic dyes, purified αFAP-PE38 protein was incubated with 50 nmol of Alexa488-TFP ester (Invitrogen) for 2 hr in 0.1 M sodium bicarbonate buffer (pH = 9.3). The unbound dye molecules were removed via buffer exchange into PBS (pH = 7.4) using a Zeba desalting spin column (Thermo Fisher Scientific). For immunofluorescent staining, the tumor samples were fixed with 4% formaldehyde, permeabilized with 0.1% Triton X-100, stained with TUNEL antibody and dye labeled αFAP-PE38, followed by counterstaining with DAPI. All fluorescence images were acquired on a Yokogawa spinning-disk confocal scanner system (Solamere Technology Group) using a Nikon eclipse Ti-E microscope (Nikon) equipped with an x60/1.49 Apo TIRF oil objective and a Cascade II: 512 EMCCD camera (Photometrics, Tucson).

In vitro cytotoxicity of αFAP-PE38

Using a commercial kit from Roche Scientific, standard XTT assays were performed to measure the dose-dependent cytotoxicity of αFAP-PE38 in cultured cells. Cells were plated on 96-well dishes one day before the treatment, followed by αFAP-PE38 treatment on day 2 and XTT assay on day 4. PBS was used as a control for 0% cell death. The OD values were normalized between the 100% cell death (0% line) and PBS controls (100% alive) and fit to a standard 4-parameter sigmoidal curve with a variable slope using the GraphPad Prism (version 5.03; GraphPad Software) program to obtain the concentration of immunotoxin at which there was 50% cell death (IC_{50}).

Tumor challenge and treatment

BALB/c mice were injected subcutaneously with 2×10^5 4T1 cells on the right flank. Treatment was started 7 days post-tumor inoculation. Paclitaxel (PTX) formulated in Cremophor/ethanol (1:1, v/v) and αFAP-PE38 diluted with 0.9% NaCl were administered to mice at the dose of 10 mg/kg and 0.5 mg/kg via i.v. injection, respectively. Tumor size was measured every two days and calculated according the following equation: volume = $(L \times S^2)/2$, where L is the long dimension and S is the short dimension. Survival end point was set when the tumor volume reached 1000 mm^3. The survival rates are presented as Kaplan-Meier curves. The survival curves of individual groups were compared by a log-rank test.

Immunohistochemical analysis

Tumor tissues were excised and fixed with 4% formaldehyde for frozen section. The sections were incubated with biotinylated anti-mouse CD31 and anti-mouse F4/80 Abs for 2 hr at room temperature, followed by incubation with streptavidin-conjugated HRP for 30 min. After incubation, the slides were washed and then developed with the DAB substrate (Abcam). After substrate development, the sections were then washed, counterstained with hematoxylin, dehydrated, and mounted with mounting medium (Richard-Allan Scientific). An *in situ* cell death detection kit (Roche) was used to detect apoptotic cells in the tumor area, following the manufacturer's instructions.

Flow cytometry analysis of TAM

Tumor tissues were harvested, minced, and then incubated with digestion buffer (RPMI supplemented with 3 mg/ml Dispase II, 1 mg/ml Collagenase I, Clostridium Histolyticum) for 30 min at 37°C. Digestion mixtures were filtered through 0.7 μm nylon strainers (BD Falcon), washed twice with cold PBS, and then incubated for 10 min at 4°C with rat anti-mouse CD16/CD32 mAb (BD Biosciences) to block nonspecific binding. Cells were then stained with anti-CD206 antibody conjugated with Alexa488 (BioLegend) and anti-F4/80 antibody conjugated with APC (BioLegend), followed by washing with PBS and fixation with 1% paraformaldehyde. Data acquisition and analysis were performed on a MACSquant cytometer using FlowJo software (Treestar Inc.).

Radiolabeling, PET imaging and biodistribution of αFAP-PE38

Radiolabeling of αFAP-PE38 was performed based on a previously reported method for AmBaSar-mediated ^{64}Cu labeling of proteins and peptides [3334]. Positron emission tomography (PET) imaging of the mice was performed using a rodent scanner (Concorde Microsystems). About 100 μCi ^{64}Cu-AmBaSar-αFAP-PE38 was diluted in a total volume of 150 μl of PBS and injected intravenously into mice bearing established 4T1 at the right flanks (n = 3). Static scans were obtained at 1, 3, and 24 hr post-injection. The images were reconstructed by a Two-Dimensional Ordered Subset Expectation Maximization (2D–OSEM) algorithm. For biodistribution, mice were sacrificed 24 hr post-injection. Tissues and organs were harvested and weighed, and the accumulated radioactivity was measured using a gamma counter. The amount of radioactivity per gram organ was given as a percentage of the total injected dose, which was arbitrarily set to 100%.

RNA isolation and transcripts analysis by qRT-PCR

Total tissue RNA was extracted from flank tumor tissues using an RNeasy Mini Kit (QIAGEN) according to the manufacturer's protocol. The cDNAs were synthesized from equal amounts of total RNAs using the SMART™ RACE cDNA Amplification Kit (BD Bioscience). Real-time qPCR with the appropriate primers was used to measure the expression of different genes. The ΔΔCt method was used to calculate change in the level of gene expression, and the raw values were normalized to the levels of the reference gene *GAPDH*.

Statistical analysis

Statistical analysis was performed by GraphPad (Prism) software to determine *P* values by Student's *t*-test where two groups were compared. When more than two groups were compared, an ANOVA with the Tukey posttest was used to determine significant differences between individual groups. Kaplan-Meier analysis was used to evaluate the survival of mice. A *P* value less than 0.05 was considered statistically significant, and data were presented as means ± SEM.

Results

Construction, purification and in vitro cytotoxicity of αFAP-PE38

The variable regions of the heavy and light chain of anti-FAP antibody (αFAP) were fused to the hinge sequence of human CD8 followed by the sequence encoding the truncated Pseudomonas exotoxin A (PE38) (Fig. S1*a*). Purified immunotoxins, migrated as a monomer in non-reducing gel (Fig. S1*b*), and SDS-PAGE analysis of the purified recombinant protein confirmed that recombinant αFAP-PE38 and PE38 proteins had the expected molecular weight of ~75 and ~48 kDa, respectively (Fig. 1*a*).

To evaluate the binding specificity of αFAP-PE38 to the target FAP, human and murine FAP-expressing cell lines were generated by stable transduction of 293T cells with lentiviral vectors encoding the human FAP (hFAP) and murine FAP (mFAP) genes, respectively. The expression of hFAP and mFAP in 293T cells was confirmed by flow cytometry analysis with anti-FAP antibody staining (Fig. 1*b*). We next analyzed the binding of immunotoxin αFAP-PE38 to the surface of hFAP- or mFAP-expressing 293T cells (293T–hFAP or 293T–mFAP). More than 94% of cells were bound with αFAP-PE38, compared with the absence of binding to negative control 293T cells (Fig. 1*c*), suggesting that the immunotoxin αFAP-PE38 binds efficiently with surface FAP in these cells.

The binding affinity of αFAP-PE38 with FAP was measured by a flow cytometry-based assay, and the K_D of the interaction between αFAP-PE38 and FAP was determined by Lineweaver-Burk kinetic analysis[33, 35]. The K_Ds of αFAP-PE38 against mFAP and hFAP were $4.68\pm0.69\times10^{-10}$ M and $1.47\pm0.7\times10^{-9}$ M, respectively, indicating that αFAP-PE38 bound to both hFAP and mFAP at high affinity (Fig.1*d*). Finally, we characterized the cytotoxic effects of αFAP-PE38 to target cells *in vitro* by performing the XTT assay (Fig. 1*e*). The immunotoxin αFAP-PE38 efficiently inhibited the viability of both 293T–hFAP and 293T–mFAP cells, with calculated IC_{50}s of 54 ng/ml and 4 ng/ml, respectively, but not that of 293T cells (Fig. 1*f*). In addition, blocking immunotoxin αFAP-PE38 binding to FAP-positive cells using excess anti-Fab antibody abolished the cell killing activity of αFAP-PE38 (Fig. S1*c*).

Biodistribution of αFAP-PE38 in 4T1 tumor-bearing mice

To test whether αFAP-PE38 specifically targets FAP-positive tumor stromal cells in *vivo*, we examined the biodistribution properties of αFAP-PE38 and PE38 in BALB/c mice bearing 4T1 tumors using positron emission tomography (PET) imaging. Static microPET scans were performed in 4T1 tumor-bearing BALB/c mice, which were injected with ^{64}Cu-AmBaSar-PE38 or ^{64}Cu-AmBaSar-αFAP-PE38 prior to imaging, at multiple time points. Accumulation of ^{64}Cu-AmBaSar-αFAP-PE38 in the tumor was observed at 1 hr after injection, and a clear tumor uptake was detected at 3 hr and 24 hr post-injection, while no obvious accumulation signal of ^{64}Cu-AmBaSar-PE38 was seen in the tumor region over the same period of time (Fig. 2*a*).

To quantify the degree of uptake on a per organ basis, we next quantitatively analyzed the biodistribution of ^{64}Cu-AmBaSar-PE38 and ^{64}Cu-AmBaSar-αFAP-PE38 in those mice at the 24 hr time point. ^{64}Cu-AmBaSar-αFAP-PE38 accumulated at 3.3-fold higher levels

than ^{64}Cu-AmBaSar-PE38 in tumors ($p<0.01$), suggesting that ^{64}Cu-AmBaSar-αFAP-PE38 was retained in 4T1 tumors by the desired targeted interaction between immunotoxins and FAP expression in the tumor mass (Fig. 2*b*). Comparable amounts of ^{64}Cu-AmBaSar-PE38 and ^{64}Cu-AmBaSar-αFAP-PE38 were detected in the liver, kidney, and spleen and, to a lesser extent, in the blood, heart, lung, small intestine and muscle. Thus, immunotoxin αFAP-PE38, but not PE38, specifically targets FAP-positive tumor stroma.

αFAP-PE38 treatment slows 4T1 breast tumor growth in vivo

To examine the antitumor efficacy of αFAP-PE38, we tested its tumor inhibition activity in a 4T1 breast carcinoma model. 4T1 cells, which are insensitive to αFAP-PE38 *in vitro* (Fig. S2), were first inoculated to the right flank of BALB/c mice to allow tumor outgrowth. Treatment was started on day 8 when the tumors reached an approximate volume of 50 mm^3. Mice were given four sequential intravenous injections with 0.5 mg/kg αFAP-PE38 or an equimolar dose of PE38 every other day for a total of 4 cycles, and tumor growth and body weights were monitored over time. Mice in the group receiving 0.5 mg/kg αFAP-PE38 showed significant retardation of tumor growth ($p<0.05$), whereas the treatment with an equimolar dose of PE38 exhibited no inhibition (Fig. 3*a*). No significant weight loss and bone marrow toxicity was seen for the duration of the experiment (Fig. S3*a* and S3*b*) and TUNEL staining of tissues, such as lung, liver, spleen and kidney (Fig. S4), which also display accumulation of immunotoxin, showed no significant difference in apoptotic index between the tissues harvested from mice treated with PE38 or αFAP-PE38, indicating that the side effects of immunotoxin αFAP-PE38, if any, were minimal.

Having shown the antitumor activity of αFAP-PE38 in a 4T1 breast carcinoma model, we next examined cell viability in tumor tissue. Tumor cells from excised tumor tissues by 7-AAD staining showed that αFAP-PE38, but not PE38, markedly reduced the number of total live cells within tumor (Fig. 3*b*). To further investigate whether the antitumor effect of αFAP-PE38 could be attributed to the induction of apoptosis, a histopathological examination was performed by *in situ* TUNEL staining. The TUNEL assay showed dramatically increased cell apoptosis in αFAP-PE38-treated tumors (23%) as compared with that in PE38-treated tumor (1.1%) (Fig. 3*c* and 3*d*). Finally, we examined if αFAP-PE38 increases TAF cell apoptosis in the tumor tissues by staining cells with TUNEL and FAP. Indeed, there are more TUNEL-positive cells among FAP-positive cells in the αFAP-PE38 treated tumors (Fig. 3*e*). Further, αFAP-PE38 treatment tumor sample displayed less expression of FAP protein (Fig. S5), indicating reduced population of FAP expressing cells within the tumor after treatment. Thus, immunotoxin αFAP-PE38 induces apoptosis of tumor stromal cells and effectively inhibits tumor growth in mice.

αFAP-PE38 treatment alters tumor microenvironment

Tumor stromal cells and infiltrating inflammatory cells produce excessive and different types of growth factors, cytokines, chemokines and matrix metalloproteinases, thereby supporting tumor growth and facilitating metastasis[2]. This prompted us to hypothesize that depletion of FAP-positive tumor stroma may alter the release of these molecules and, consequently, change the tumor microenvironment. To test this hypothesis, we first investigated their mRNA and protein expression in 4T1 tumor tissues collected from αFAP-

PE38-treated or PE38-treated control mice (Fig. 4*a* and Fig. S6). Consistent with a previous study[10], the expression of TNF-α was significantly increased in the αFAP-PE38-treated tumor. The expression of proinflammatory cytokine TGF-β, which has been implicated in many aspects of tumorigenesis by directly acting on the tumor cell, as well as influencing the tumor microenvironment[36, 37], was significantly reduced upon αFAP-PE38 treatment. MMPs and VEGF play important roles in vasculogenesis and angiogenesis[38]. Immunotoxin αFAP-PE38 reduced the expression of VEGF and MMP-9, but not MMP-2. It also downregulated the expression of chemokines CCL5, MCP-1 and SDF-1. Consistent with the downregulation of CCL5 and MCP-1, both of which can mediate the recruitment of macrophage cells[11, 39], we observed a dramatic decrease of the F4/80$^+$/CD206$^+$ tumor-associated macrophage (TAM) population in αFAP-PE38-treated tumors, as compared with the PE38-treated tumors (16.8% versus 5.7%, $p<0.05$) (Fig. 4*b* and 4*c*). Thus, immunotoxin αFAP-PE38 alters the levels of growth factors, cytokines, chemokines and matrix metalloproteinases and inhibits the recruitment of TAMs.

Combined αFAP-PE38 and paclitaxel therapy increases antitumor activity

It is well accepted that macromolecules, such as antibody immunotoxins, immunocytokines, and other immunoconjugates, enter solid tumors slowly because of the diffusion barrier. Cytotoxic chemotherapy agents, such as paclitaxel and cyclophosphamide, can "sensitize" the tumor to the tumoricidal effects of the immunocytokine in the tumor microenvironment, likely by increasing the uptake of immunotcyokine into tumors[40, 41]. We next investigated the effectiveness of the combination treatment with αFAP-PE38 and paclitaxel. The mice bearing 4T1 tumors were treated with vehicle, two doses of paclitaxel (10 mg/kg) alone every seven days, six doses of αFAP-PE38 (0.5 mg/kg) alone every other day, or both αFAP-PE38 and paclitaxel. When both agents were used, paclitaxel was given 1 day before the first dose of αFAP-PE38. Mice receiving the combination of αFAP-PE38 and paclitaxel treatments showed a significantly reduced mean tumor volume (418±77 mm^3) compared with mice receiving αFAP-PE38 alone (770±122 mm^3, $p<0.01$), paclitaxel alone (684±56.2 mm^3, $p<0.05$), or untreated group (1194±62.7 mm^3, $p<0.001$) (Fig. 5*a*, left panel). Further, the survival study showed that the groups that received the combination treatment had a median survival of 35 days and lived significantly longer than mice treated with either agent alone (log-rank $p<0.05$) or those in the control group (log-rank $p<0.001$) (Fig. 5*a*, right panel).

Angiogenesis is critical for invasive tumor growth and metastasis[42]. We next evaluated the effects of αFAP-PE38 on angiogenesis by performing immunohistochemical staining of CD31, which is a superior vascular marker for angiogenesis, on the 4T1 tumors. αFAP-PE38 and paclitaxel alone inhibited angiogenesis in 4T1 tumors, as shown by the significantly decreased vascular density in those tumors (Fig. 5*b* and 5*c*). Importantly, combined treatment with αFAP-PE38 and paclitaxel virtually abrogated the angiogenesis in 4T1 tumors. In addition, we observed a dramatic decrease in the F4/80$^+$/CD206$^+$ macrophage population in 4T1 tumors treated by αFAP-PE38 alone ($p<0.001$), but not paclitaxel alone. Combined treatment with paclitaxel did not show further decrease of macrophage population, as compared with αFAP-PE38 treatment only (Fig. 5*b* and 5*d*).

Thus, combinatorial therapy with αFAP-PE38 and paclitaxel inhibits angiogenesis and increases antitumor activity.

Discussion

In this study, we developed a novel FAP-targeting immunotoxin, αFAP-PE38, to target FAP-expressing stromal cells. We have constructed and purified recombined immunotoxin αFAP-PE38 and demonstrated that it bound with FAP at high affinity. Using XTT assays, we have shown that αFAP-PE38 specifically killed cell lines constitutively expressing FAP. In addition, we have also used PET imaging to show the targeting of αFAP-PE38 to FAP-positive tumor stroma in mice. Furthermore, we have shown that depletion of FAP-positive stromal cells reduced tumor growth by inhibiting angiogenesis and inducing apoptosis, with altered levels of various growth factors, cytokines, chemokines and matrix metalloproteinases in the tumor microenvironment and a concomitant decreased recruitment of TAMs. Finally, we have shown that paclitaxel enhanced the antitumor activity of αFAP-PE38 in mice.

Tumor stromal cells represent a reservoir of potential chemotherapeutic targets [43]. Strategies that endeavor to exploit cellular targets within the tumor stromal cells offer several potential advantages over traditional approaches. First, the target is more genetically stable and thus less likely to acquire resistance to a cytotoxic agent. Second, many solid tumor malignancies share common alterations in their tumor microenvironment; therefore, approaches that target these alterations may be widely applied to many of these tumors.

FAP is highly expressed on the surface of fibroblasts in the stroma of many epithelial cancers and has emerged as a promising target for cancer treatment[12, 18]. In our study, we have adopted a more viable strategy by using the novel immunotoxin αFAP-PE38 to specifically target FAP-expressing stroma cells. Independent of the potentially uncertain role of FAP in tumorigenesis, this strategy would be effective since the therapeutic effect of αFAP-PE38 relies on stroma-restricted distribution of FAP, rather than strictly on inhibition of its function. In addition to the restricted distribution of FAP in stroma, efficient internalization of an antibody upon binding is a prerequisite for FAP in targeted therapy. Our data showed that αFAP-PE38 bound to the cell-surface expressed FAP antigen with high affinity. Importantly, depletion of tumor stromal cells by αFAP-PE38 results in significant inhibition of tumor growth in a mouse model and prolongs survival in a tumor challenge assay. The ability of αFAP-PE38 to target tumor microenvironment is confirmed by our biodistribution study showing that αFAP-PE38 was significantly accumulated at tumor sites, as compared with that of PE38 (Fig. 2), and our immunofluorescence staining showing that the majority of apoptotic cells in αFAP-PE38-treated tumor were FAP-expressing tumor stroma (Fig 3*e*).

The tumor and its microenvironment exist in a dynamic and interconnected network of reciprocal interactions that can influence cell proliferation, survival, migration, invasion and angiogenesis[44, 45]. Such effects are mediated via both paracrine and autocrine stimulation by a variety of growth factors, cytokines, chemokines and matrix metalloproteinases. αFAP-PE38 treatment reduced the recruitment of infiltrating TAMs, decreased angiogenesis to

deprive tumor cells of required nutrients and oxygen, and inhibited tumor cell growth, suggesting that elimination of the FAP-expressing population could lead to an antitumor effect through multiple mechanisms. Such effects are likely mediated through altering the tumor microenvironment, as suggested by the altered expression of TNF-α, TGF-β, CCL5, MCP-1, SDF-1, VEGF and MMPs, upon αFAP-PE38 treatment (Fig 4*a*). Decreased angiogenesis upon αFAP-PE38 treatment is likely due to both reduced TAFs and infiltrating TAMs, which can both release of angiogenic molecules, such as VEGFs. In fact, one key aspect of tumor stroma formation in solid neoplasms is the production of new blood vessels (angiogenesis) to provide an enhanced tumor blood[46]. Our finding that αFAP-PE38 immunotoxin significantly reduces TAFs and TAMs, and subsequent the level of VEGF, which regulates blood vessel growth and maturation[47, 48], suggest that αFAP-PE38 immunotoxin treatment could likely prevent development of vessels.

Consistent with several previous preclinical studies targeting FAP, in which no significant toxicities were reported[10, 49–51], αFAP-PE38 treatment does not result in significant off-target toxicity. However, Tran and his colleagues reported bone toxicity and cachexia upon immune targeting of FAP-expressing cells using FAP5-CAR-transduced T cells[52]. Such discrepancy between this study and ours' is likely due to differences in the mechanism of FAP-targeting therapies. For example, the antitumor T cell response mediated by adoptively transferred T cells is more robust and these T cells likely circulate in the body for longer time than targeting immunotoxin, which typically have maximal half-life of several hours[28]. It is also possible that the high dose is associated with significant toxicity in their study as they also found that the majority of those mice treated with 5×10^6 FAP5-CAR-transduced T cells did not succumb to treatment-related toxicities.

Despite recent advances in chemotherapeutic agents for cancer, their clinical applications are often limited by systemic toxicity. The combined use of an immunotoxin and a chemotherapeutic agent could provide a new strategy to not only minimize potential systemic toxicity but also maximize efficacy. Our data showed that mice treated with a combination of αFAP-PE38 and paclitaxel displayed a significantly increased inhibition of tumor growth and prolonged survival as compared to that of either agent alone, and no obvious systemic toxicity was observed. It is likely that the enhanced antitumor activity of combined treatment can be attributed, at least in part, to increased "uptake" of immunotoxin αFAP-PE38 by stroma cells. It is also possible that the direct immunosuppressive properties of paclitaxel may decrease formation of neutralizing antibodies to immunotoxins and, therefore, enhances anti-tumor activity. The combined treatment resulted in a significant inhibition of angiogenesis, but not the recruitment of TAMs, suggesting that modulation of angiogenesis may be one of the important mechanisms underpinning the enhanced antitumor activity of combined therapy.

Taken together, our findings provide the rationale for using FAP-targeting immunotoxin to deplete FAP-expressing TAFs and demonstrate the feasibility of using this immunotoxin to inhibit tumor growth *in vivo*, thus paving the way for applying this potent and selective FAP-targeting immunotoxin for cancer therapy. During the treatment with immunotoxins, the early production of neutralizing antibodies to immunotoxins is one of the major limiting factors for their efficacy. Recent study has identified eight helper T-cell epitopes, which are

required for T-cell activation and subsequent generation of neutralizing antibodies against PE38[53]. It will be interesting to make new αFAP-PE38, in which three epitopes were deleted and five others diminished by point mutations, and to exam if this modification will yield better antitumor activity.

Supplementary Material

Refer to Web version on PubMed Central for supplementary material.

Acknowledgements

This work was supported by National Institutes of Health grants (R01AI068978, R01CA170820, R01EB017206 and P01CA132681), a translational acceleration grant from the Joint Center for Translational Medicine, the National Cancer Institute (P30CA014089), and a grant from the Ming Hsieh Institute for Research on Engineering Medicine for Cancer.

References

1. Tlsty TD, Coussens LM. Tumor stroma and regulation of cancer development. Annu Rev Pathol. 2006; 1:119–150. [PubMed: 18039110]
2. Bhowmick NA, Neilson EG, Moses HL. Stromal fibroblasts in cancer initiation and progression. Nature. 2004; 432:332–337. [PubMed: 15549095]
3. Kalluri R, Zeisberg M. Fibroblasts in cancer. Nat Rev Cancer. 2006; 6:392–401. [PubMed: 16572188]
4. Balkwill F. Tumor necrosis factor or tumor promoting factor? Cytokine Growth Factor Rev. 2002; 13:135–141. [PubMed: 11900989]
5. Balkwill F. Cancer and the chemokine network. Nat Rev Cancer. 2004; 4:540–550. [PubMed: 15229479]
6. Kessenbrock K, Plaks V, Werb Z. Matrix metalloproteinases: regulators of the tumor microenvironment. Cell. 2010; 141:52–67. [PubMed: 20371345]
7. Singer CF, Kronsteiner N, Marton E, Kubista M, Cullen KJ, Hirtenlehner K, Seifert M, Kubista E. MMP-2 and MMP-9 expression in breast cancer-derived human fibroblasts is differentially regulated by stromal-epithelial interactions. Breast Cancer Res Treat. 2002; 72:69–77. [PubMed: 12000221]
8. Roomi MW, Monterrey JC, Kalinovsky T, Rath M, Niedzwiecki A. Patterns of MMP-2 and MMP-9 expression in human cancer cell lines. Oncol Rep. 2009; 21:1323–1333. [PubMed: 19360311]
9. Kojima Y, Acar A, Eaton EN, Mellody KT, Scheel C, Ben-Porath I, Onder TT, Wang ZC, Richardson AL, Weinberg RA, Orimo A. Autocrine TGF-beta and stromal cell-derived factor-1 (SDF-1) signaling drives the evolution of tumor-promoting mammary stromal myofibroblasts. Proc Natl Acad Sci U S A. 2010; 107:20009–200014. [PubMed: 21041659]
10. Kraman M, Bambrough PJ, Arnold JN, Roberts EW, Magiera L, Jones JO, Gopinathan A, Tuveson DA, Fearon DT. Suppression of antitumor immunity by stromal cells expressing fibroblast activation protein-alpha. Science. 2010; 330:827–830. [PubMed: 21051638]
11. Mishra P, Banerjee D, Ben-Baruch A. Chemokines at the crossroads of tumor-fibroblast interactions that promote malignancy. J Leukoc Biol. 2011; 89:31–39. [PubMed: 20628066]
12. Liu R, Li H, Liu L, Yu J, Ren X. Fibroblast activation protein: A potential therapeutic target in cancer. Cancer Biol Ther. 2012; 13:123–129. [PubMed: 22236832]
13. Kakarla S, Chow K, Mata M, Shaffer DR, Song XT, Wu MF, Liu H, Wang LL, Rowley DR, Pfizenmaier K, Gottschalk S. Antitumor effects of chimeric receptor engineered human T cells directed to tumor stroma. Molecular therapy : the journal of the American Society of Gene Therapy. 2013; 21:1611–1620. [PubMed: 23732988]

14. Brennen WN, Rosen DM, Wang H, Isaacs JT, Denmeade SR. Targeting carcinoma-associated fibroblasts within the tumor stroma with a fibroblast activation protein-activated prodrug. Journal of the National Cancer Institute. 2012; 104:1320–1334. [PubMed: 22911669]
15. Tuxhorn JA, Ayala GE, Smith MJ, Smith VC, Dang TD, Rowley DR. Reactive stroma in human prostate cancer: induction of myofibroblast phenotype and extracellular matrix remodeling. Clin Cancer Res. 2002; 8:2912–2923. [PubMed: 12231536]
16. Santos AM, Jung J, Aziz N, Kissil JL, Pure E. Targeting fibroblast activation protein inhibits tumor stromagenesis and growth in mice. J Clin Invest. 2009; 119:3613–3625. [PubMed: 19920354]
17. Kelly T, Huang Y, Simms AE, Mazur A. Fibroblast activation protein-alpha: a key modulator of the microenvironment in multiple pathologies. Int Rev Cell Mol Biol. 2012; 297:83–116. [PubMed: 22608558]
18. Brennen WN, Isaacs JT, Denmeade SR. Rationale behind targeting fibroblast activation protein-expressing carcinoma-associated fibroblasts as a novel chemotherapeutic strategy. Molecular cancer therapeutics. 2012; 11:257–266. [PubMed: 22323494]
19. Jacob M, Chang L, Pure E. Fibroblast activation protein in remodeling tissues. Current molecular medicine. 2012; 12:1220–1243. [PubMed: 22834826]
20. Huang Y, Simms AE, Mazur A, Wang S, Leon NR, Jones B, Aziz N, Kelly T. Fibroblast activation protein-alpha promotes tumor growth and invasion of breast cancer cells through non-enzymatic functions. Clin Exp Metastasis. 2011; 28:567–579. [PubMed: 21604185]
21. Lee HO, Mullins SR, Franco-Barraza J, Valianou M, Cukierman E, Cheng JD. FAP-overexpressing fibroblasts produce an extracellular matrix that enhances invasive velocity and directionality of pancreatic cancer cells. BMC Cancer. 2011; 11:245. [PubMed: 21668992]
22. Cheng JD, Valianou M, Canutescu AA, Jaffe EK, Lee HO, Wang H, Lai JH, Bachovchin WW, Weiner LM. Abrogation of fibroblast activation protein enzymatic activity attenuates tumor growth. Molecular cancer therapeutics. 2005; 4:351–360. [PubMed: 15767544]
23. Wolf BB, Quan C, Tran T, Wiesmann C, Sutherlin D. On the edge of validation--cancer protease fibroblast activation protein. Mini Rev Med Chem. 2008; 8:719–727. [PubMed: 18537727]
24. Narra K, Mullins SR, Lee HO, Strzemkowski-Brun B, Magalong K, Christiansen VJ, McKee PA, Egleston B, Cohen SJ, Weiner LM, Meropol NJ, Cheng JD. Phase II trial of single agent Val-boroPro (Talabostat) inhibiting Fibroblast Activation Protein in patients with metastatic colorectal cancer. Cancer Biol Ther. 2007; 6:1691–1699. [PubMed: 18032930]
25. Tsai TY, Yeh TK, Chen X, Hsu T, Jao YC, Huang CH, Song JS, Huang YC, Chien CH, Chiu JH, Yen SC, Tang HK, et al. Substituted 4-carboxymethylpyroglutamic acid diamides as potent and selective inhibitors of fibroblast activation protein. J Med Chem. 2010; 53:6572–6583. [PubMed: 20718420]
26. Walsh MP, Duncan B, Larabee S, Krauss A, Davis JP, Cui Y, Kim SY, Guimond M, Bachovchin W, Fry TJ. Val-boroPro accelerates T cell priming via modulation of dendritic cell trafficking resulting in complete regression of established murine tumors. PloS one. 2013; 8:e58860. [PubMed: 23554941]
27. Pastan I, Hassan R, Fitzgerald DJ, Kreitman RJ. Immunotoxin therapy of cancer. Nat Rev Cancer. 2006; 6:559–565. [PubMed: 16794638]
28. Pastan I, Hassan R, FitzGerald DJ, Kreitman RJ. Immunotoxin treatment of cancer. Annu Rev Med. 2007; 58:221–237. [PubMed: 17059365]
29. Kioi M, Seetharam S, Puri RK. Targeting IL-13Ralpha2-positive cancer with a novel recombinant immunotoxin composed of a single-chain antibody and mutated Pseudomonas exotoxin. Molecular cancer therapeutics. 2008; 7:1579–1587. [PubMed: 18566228]
30. Madhumathi J, Verma RS. Therapeutic targets and recent advances in protein immunotoxins. Curr Opin Microbiol. 2012; 15:300–309. [PubMed: 22647353]
31. Yang L, Yang H, Rideout K, Cho T, Joo KI, Ziegler L, Elliot A, Walls A, Yu D, Baltimore D, Wang P. Engineered lentivector targeting of dendritic cells for in vivo immunization. Nature biotechnology. 2008; 26:326–334.
32. Brocks B, Garin-Chesa P, Behrle E, Park JE, Rettig WJ, Pfizenmaier K, Moosmayer D. Species-crossreactive scFv against the tumor stroma marker “fibroblast activation protein” selected by

phage display from an immunized FAP−/− knock-out mouse. Molecular medicine. 2001; 7:461–469. [PubMed: 11683371]

33. Xiao L, Hung KC, Takahashi TT, Joo KI, Lim M, Roberts RW, Wang P. Antibody-Mimetic Ligand Selected by mRNA Display Targets DC-SIGN for Dendritic Cell-Directed Antigen Delivery. ACS chemical biology. 2013; 8:967–977. [PubMed: 23427768]
34. Li Z, Jin Q, Huang C, Dasa S, Chen L, Yap LP, Liu S, Cai H, Park R, Conti PS. Trackable and Targeted Phage as Positron Emission Tomography (PET) Agent for Cancer Imaging. Theranostics. 2011; 1:371–380. [PubMed: 22211143]
35. Benedict CA, MacKrell AJ, Anderson WF. Determination of the binding affinity of an anti-CD34 single-chain antibody using a novel, flow cytometry based assay. Journal of immunological methods. 1997; 201:223–231. [PubMed: 9050944]
36. Mocellin S, Marincola FM, Young HA. Interleukin-10 and the immune response against cancer: a counterpoint. J Leukoc Biol. 2005; 78:1043–1051. [PubMed: 16204623]
37. Connolly EC, Freimuth J, Akhurst RJ. Complexities of TGF-beta targeted cancer therapy. International journal of biological sciences. 2012; 8:964–978. [PubMed: 22811618]
38. Ferrara N, Kerbel RS. Angiogenesis as a therapeutic target. Nature. 2005; 438:967–974. [PubMed: 16355214]
39. Keophiphath M, Rouault C, Divoux A, Clement K, Lacasa D. CCL5 promotes macrophage recruitment and survival in human adipose tissue. Arteriosclerosis, thrombosis, and vascular biology. 2010; 30:39–45.
40. Holden SA, Lan Y, Pardo AM, Wesolowski JS, Gillies SD. Augmentation of antitumor activity of an antibody-interleukin 2 immunocytokine with chemotherapeutic agents. Clin Cancer Res. 2001; 7:2862–2869. [PubMed: 11555604]
41. Zhang Y, Xiang L, Hassan R, Paik CH, Carrasquillo JA, Jang BS, Le N, Ho M, Pastan I. Synergistic antitumor activity of taxol and immunotoxin SS1P in tumor-bearing mice. Clin Cancer Res. 2006; 12:4695–4701. [PubMed: 16899620]
42. Folkman J. Role of angiogenesis in tumor growth and metastasis. Seminars in oncology. 2002; 29:15–18. [PubMed: 12516034]
43. Hofmeister V, Schrama D, Becker JC. Anti-cancer therapies targeting the tumor stroma. Cancer immunology, immunotherapy : CII. 2008; 57:1–17. [PubMed: 17661033]
44. Albini A, Sporn MB. The tumour microenvironment as a target for chemoprevention. Nat Rev Cancer. 2007; 7:139–147. [PubMed: 17218951]
45. Swartz MA, Iida N, Roberts EW, Sangaletti S, Wong MH, Yull FE, Coussens LM, DeClerck YA. Tumor microenvironment complexity: emerging roles in cancer therapy. Cancer research. 2012; 72:2473–2480. [PubMed: 22414581]
46. Hanahan D, Folkman J. Patterns and emerging mechanisms of the angiogenic switch during tumorigenesis. Cell. 1996; 86:353–364. [PubMed: 8756718]
47. Conway EM, Collen D, Carmeliet P. Molecular mechanisms of blood vessel growth. Cardiovascular research. 2001; 49:507–521. [PubMed: 11166264]
48. Jain RK. Molecular regulation of vessel maturation. Nature medicine. 2003; 9:685–693.
49. Loeffler M, Kruger JA, Niethammer AG, Reisfeld RA. Targeting tumor-associated fibroblasts improves cancer chemotherapy by increasing intratumoral drug uptake. J Clin Invest. 2006; 116:1955–1962. [PubMed: 16794736]
50. Liao D, Luo Y, Markowitz D, Xiang R, Reisfeld RA. Cancer associated fibroblasts promote tumor growth and metastasis by modulating the tumor immune microenvironment in a 4T1 murine breast cancer model. PloS one. 2009; 4:e7965. [PubMed: 19956757]
51. Wen Y, Wang CT, Ma TT, Li ZY, Zhou LN, Mu B, Leng F, Shi HS, Li YO, Wei YQ. Immunotherapy targeting fibroblast activation protein inhibits tumor growth and increases survival in a murine colon cancer model. Cancer science. 2010; 101:2325–2332. [PubMed: 20804499]
52. Tran E, Chinnasamy D, Yu Z, Morgan RA, Lee CC, Restifo NP, Rosenberg SA. Immune targeting of fibroblast activation protein triggers recognition of multipotent bone marrow stromal cells and cachexia. The Journal of experimental medicine. 2013; 210:1125–1135. [PubMed: 23712432]
53. Mazor R, Eberle JA, Hu X, Vassall AN, Onda M, Beers R, Lee EC, Kreitman RJ, Lee B, Baker D, King C, Hassan R, et al. Recombinant immunotoxin for cancer treatment with low

immunogenicity by identification and silencing of human T-cell epitopes. Proc Natl Acad Sci U S A. 2014; 111:8571–8576. [PubMed: 24799704]

What's new?

As a key component of tumor stroma, tumor-associated fibroblasts (TAFs) promote malignant growth, angiogenesis, invasion and metastasis. Fibroblast activation protein (FAP), a surface protein that is exceedingly expressed in TAFs, could function as an attractive target for cancer therapy in a broad range of cancers. In this study, the authors developed a novel immunotoxin αFAP-PE38 targeting the non-malignant compartment of solid tumors and demonstrated its potent anti-tumor activity as well as the enhanced therapeutic efficacy of this immunotoxin with paclitaxel. These studies pave the way for applying the combination of FAP-targeting immunotoxin and chemotherapeutic agent as a promising new strategy to enhance clinical application of immunotoxin-based therapies.

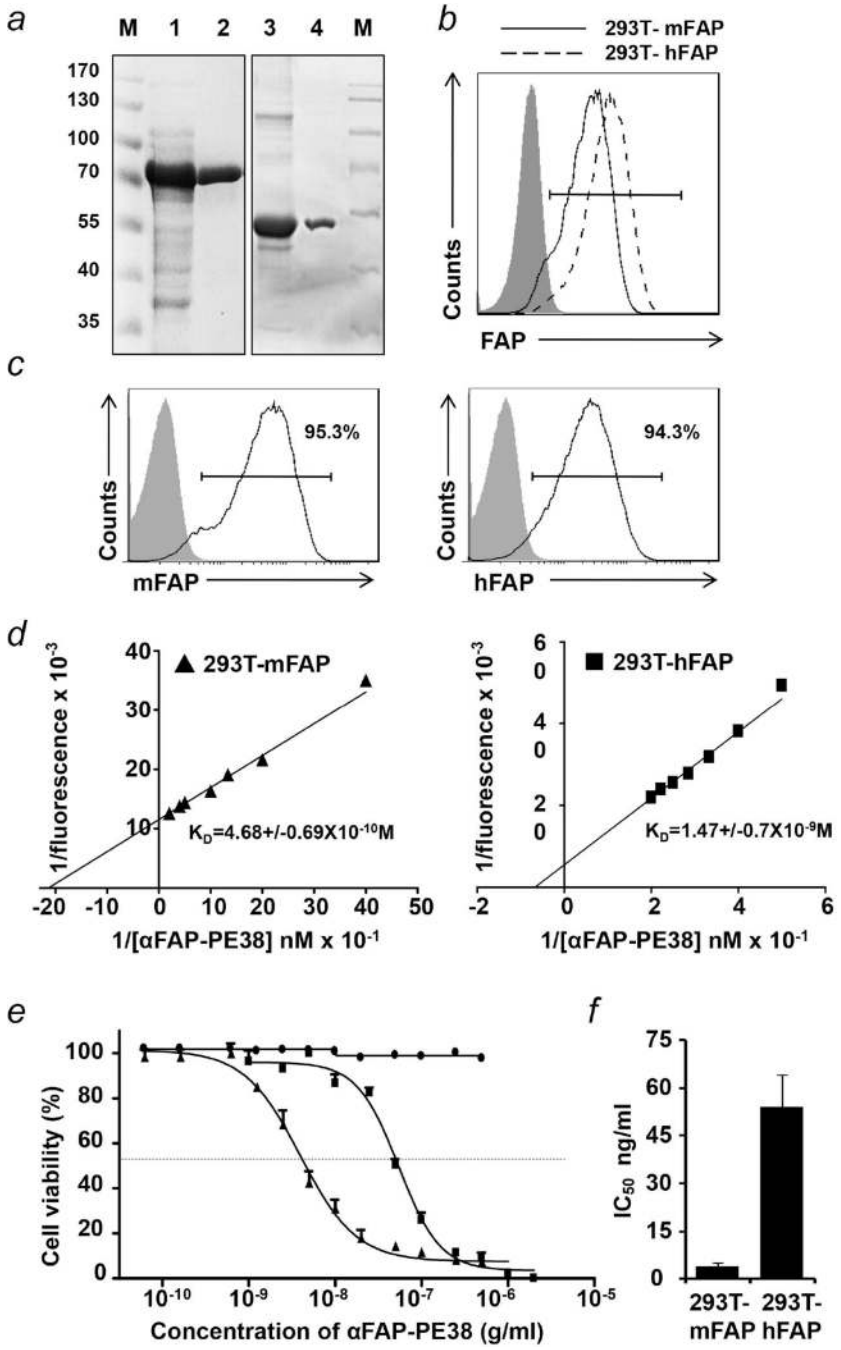

Figure 1. Preparation and characterization of recombinant anti-FAP immunotoxin

(*a*) SDS-PAGE of purified immunotoxins. Lane 1, inclusion bodies containing αFAP-PE38 from *Escherichia coli* in 8M urea; Lane 2, purified αFAP-PE38 after His-tag affinity chromatography; Lane 3, PE38 inclusion bodies; Lane 4, purified PE38 after His-tag affinity chromatography. (*b*) FACS analysis of hFAP or mFAP expressing on 293T cells. The VSVG-pseudotyped lentiviral vectors FUW-hFAP and FUW-mFAP were used to transduce 293T cells and the stable transduced cells 293T–hFAP and 293T–mFAP were stained with anti-FAP antibody for analysis of FAP expression by FACS. 293T was used as negative

control (shaded area). (*c*) FACS analysis of immunotoxin αFAP-PE38 binding to 293T control (shaded area) or 293T–mFAP/293T–hFAP (solid line) cells. (*d*) The K_D value of the interaction between αFAP-PE38 and cell-surface mFAP/hFAP, as determined by Lineweaver-Burk analysis. (*e*) The cell cytotoxicity of αFAP-PE38 against 293T, 293T–mFAP and 293T–hFAP cells was performed by a standard XTT assay with a 48 hr treatment procedure. (*f*) Summary of cytotoxic activity of αFAP-PE38 on 293T–mFAP and 293T–hFAP cells. Data are given as an IC_{50} value, the concentration of immunotoxin that causes a 50% inhibition of cell death after a 48-hour incubation with immunotoxin. All the assays were conducted in triplicate for each cell line. Data are representative of mean ± SEM.

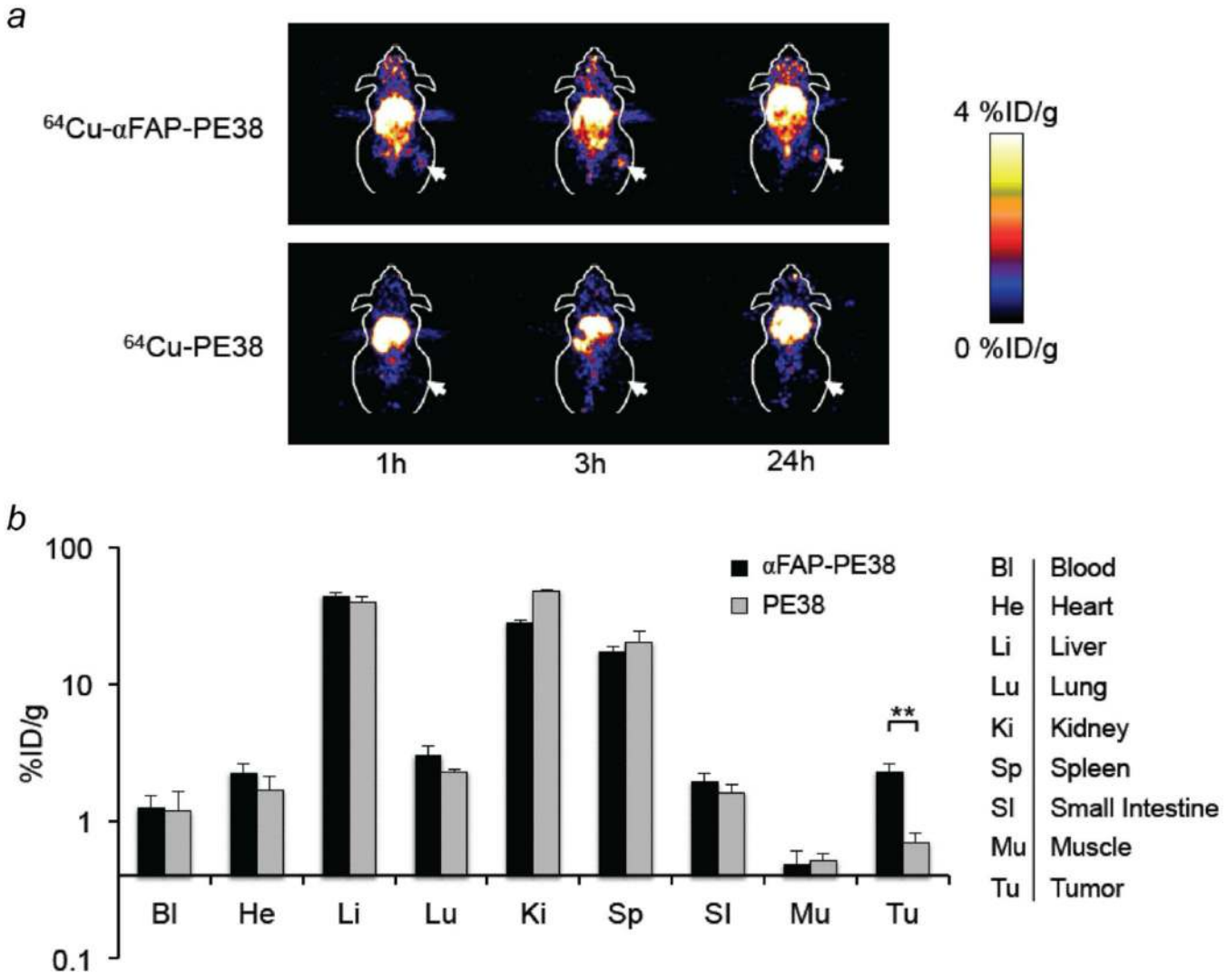

Figure 2. Imaging and Biodistribution of ^{64}Cu-labeled αFAP-PE38

(*a*) *In vivo* PET images of mice bearing 4T1 tumors at 1h, 3h and 24h after i.v. injection of ^{64}Cu-AmBaSar-αFAP-PE38 or ^{64}Cu-AmBaSar-PE38. An obvious accumulation of ^{64}Cu-αFAP-PE38 in tumor was observed 1 hr after administration. Mice injected with ^{64}Cu-AmBaSar-PE38 showed no prominent accumulation in tumor (n = 3/group). (*b*) Biodistribution of αFAP-PE38 and PE38 in different tissues at 24 hr after injection with ^{64}Cu-AmBaSar-αFAP-PE38 or ^{64}Cu-AmBaSar-PE38 shown as percentage of injection dose per g of tissues (% ID/g). Tumor uptake was significantly higher in the mice injected with ^{64}Cu-αFAP-PE38, as compared to the mice injected with ^{64}Cu-PE38 (**: $p<0.01$). Data are representative of two independent experiments.

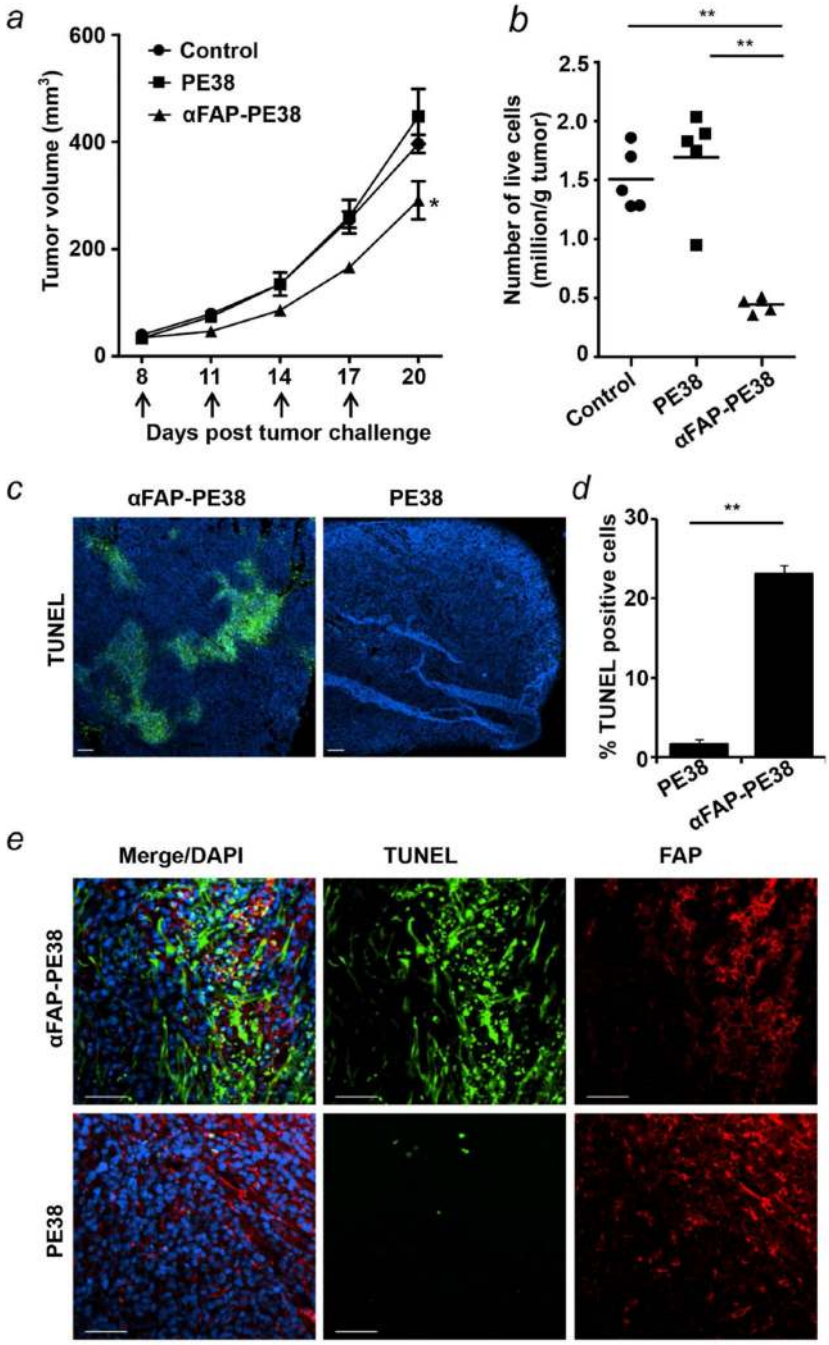

Figure 3. Antitumor efficacy of αFAP-PE38 in 4T1 tumor-bearing mice

(*a*) Effect of αFAP-PE38 on the growth of established 4T1 breast cancer model. Female BALB/c mice were inoculated s.c. with 2×10^5 4T1 cells in the right flank and then treated with vehicle, αFAP-PE38 (0.5 mg/kg) or PE38 (0.5 mg/kg) 7 days after tumor implantation through i.v. injection for total four time at the indicated days. Tumor volume was monitored every 3 days post-initiation of the treatment. Error bars, average tumor volume ± SEM, n = 5 for each treatment group. (*b*) Percentage of viable cells of isolated tumor from αFAP-PE38- and PE38-treated mice. Tumor tissue harvested from treated mice was minced and

digested into single cell suspension. The cells were then filtered through 0.7 μm nylon strainers, washed twice with cold PBS, and stained with 7-AAD. (*c*) Representative images of apoptosis in tumor sections. Cell apoptosis was detected by TUNEL staining (nuclei stained with DAPI, blue; apoptotic cells stained with FITC, green). (*d*) Quantification of TUNEL-positive cells represented in (*c*). Four regions of interest (ROI) were randomly chosen per image at 10 magnification and areas of TUNEL-positive nuclei and areas of nuclear staining were counted per region. Data were depicted as mean TUNEL-positive% area fraction ± SEM (n=3). (*e*) FAP-positive stromal cells (red) undergo apoptosis as indicated by TUNEL-positive nuclei (green) following treatment with αFAP-PE38 (upper panel), but not PE38 (bottom panel). Dye labeled αFAP-PE38 was used to detect FAP expression on the tumor section. (*: $p<0.05$; **: $p<0.01$). Data are representative of three independent experiments.

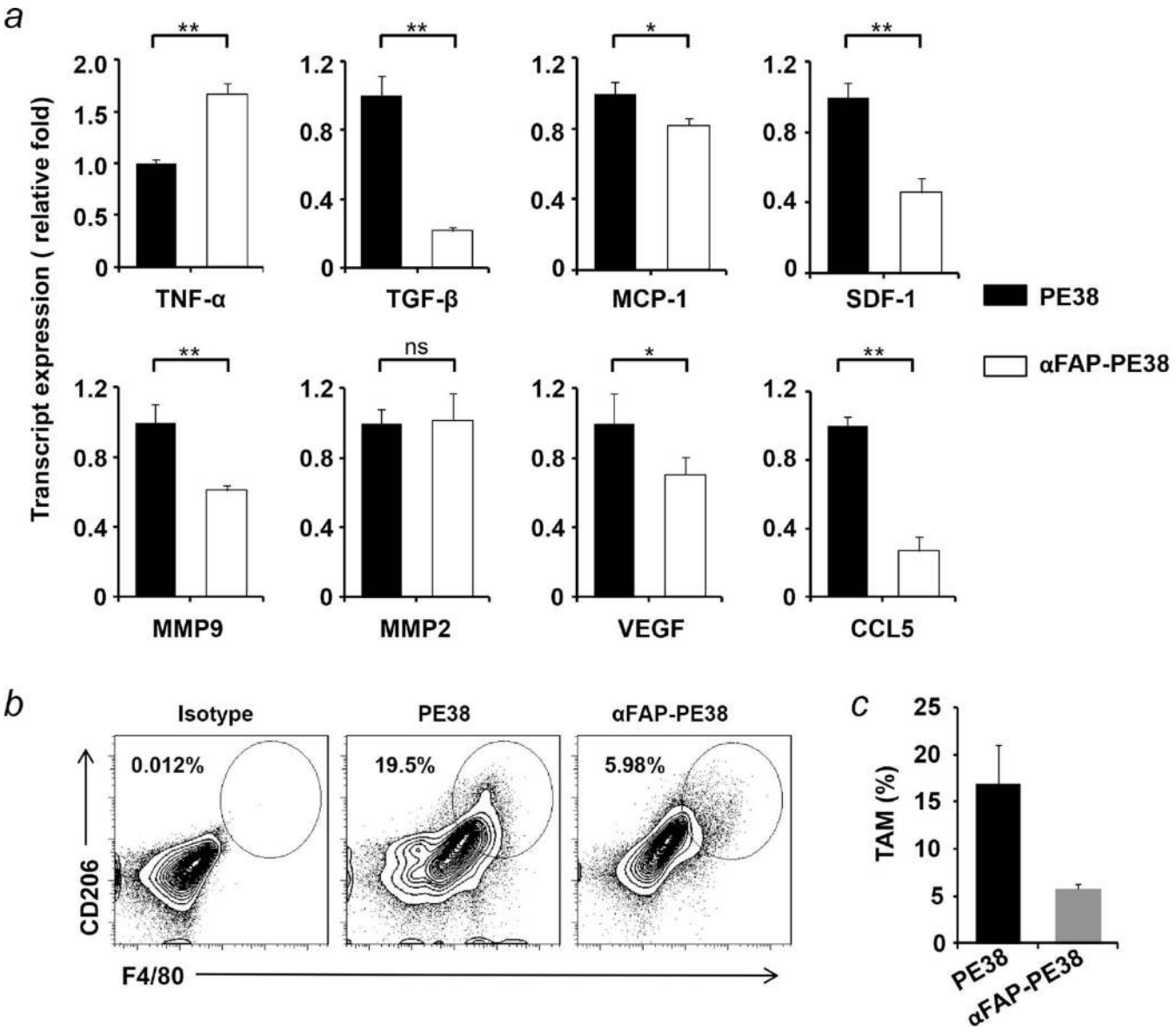

Figure 4. Targeting of FAP-expressing cells results in decreasing TAM population in tumor and altering the release of cytokines, chemokines, growth factors and matrix metalloproteinases

(a) Relative mRNA levels of cytokines and growth factors in 4T1 tumors from tumor-bearing BALB/c mice receiving 4 i.v. injections of αFAP-PE38 or PE38. Data were normalized to the expression of *GAPDH* and were depicted as mean fold change of gene expression in αFAP-PE38-treated tumors compared to those in PE38-treated tumors. Each bar is the mean of triplicate measurement for three mice. Data are representative of mean ± SEM (*: p<0.05; **: p<0.01). (*b*) Representative flow cytometry plots of the population of $CD206^{+}F4/80^{+}$ tumor-associated macrophages (TAMs) in 4T1 tumor tissues harvested from αFAP-PE38- and PE38-treated mice. (*c*) The percentage of TAMs in 4T1 tumor tissues harvested from αFAP-PE38- and PE38-treated mice. Data are representative of mean ± SEM (*: p<0.05). Data are representative of three independent experiments.

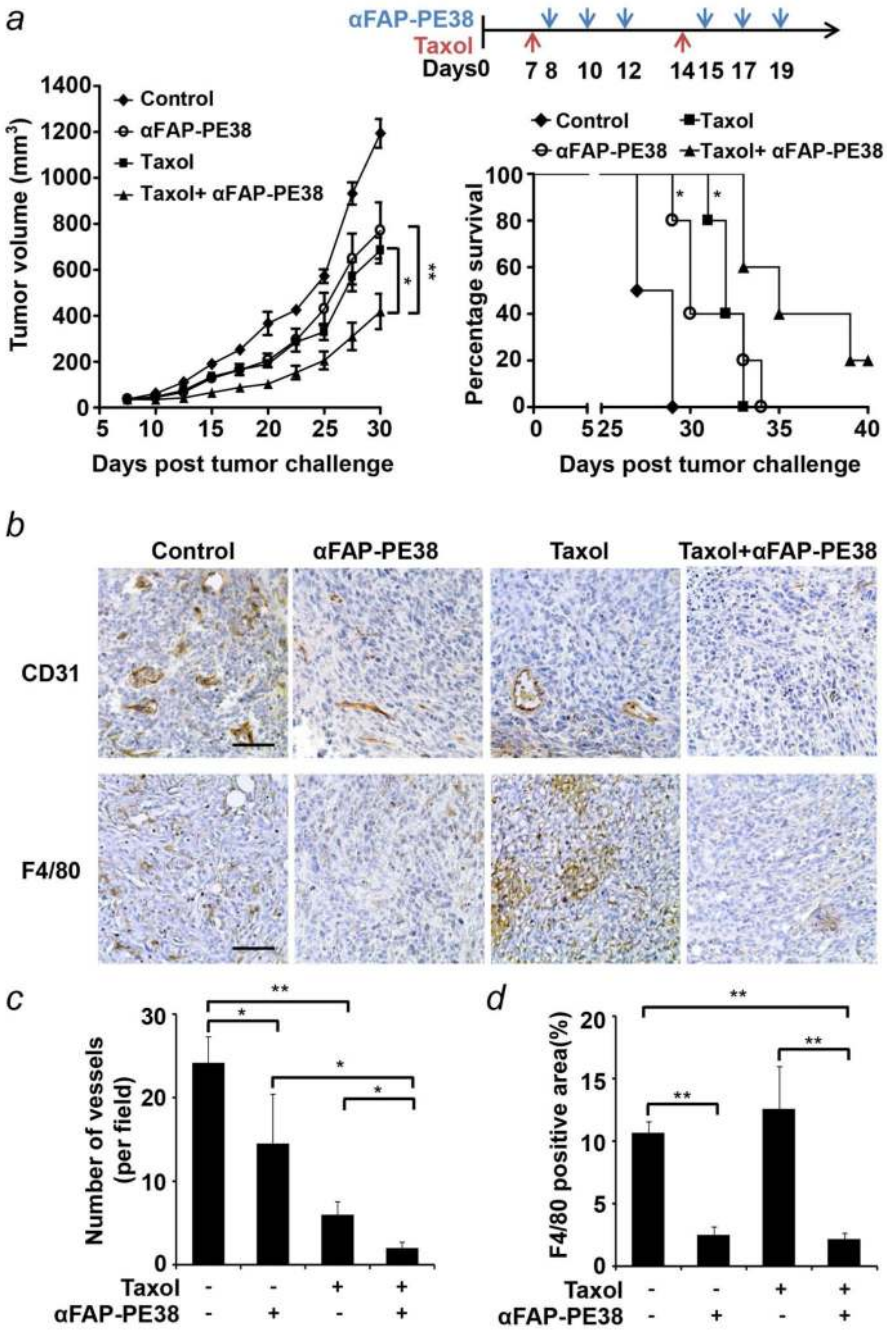

Figure 5. Combined treatment with αFAP-PE38 and paclitaxel displays enhanced antitumor activity

(*a*) Inhibition of tumor growth by treatment with immunotoxin in combination with chemotherapy. Mice were inoculated s.c. with 2×10^5 4T1 cells in the right flank and treated with paclitaxel (PTX) 10mg/kg, αFAP-PE38 0.5mg/kg, or the combination of both agents through i.v. injection. Treatment regimens are depicted for all groups. The tumor volume was assessed every 3 days and data are displayed as mean tumor volume ± SEM (n = 6 mice/group). αFAP-PE38/PTX versus αFAP-PE38, $p<0.01$; versus PTX, $p<0.05$; versus untreated, $p<0.001$. Mice received αFAP-PE38/PTX treatment demonstrated a significantly

prolonged survival than mice received αFAP-PE38 or PTX alone (*: $p<0.05$, Kaplan–Meier survival analysis). (*b*) Immunohistochemical analysis of 4T1 tumors harvested from untreated mice or mice treated with αFAP-PE38 alone, PTX alone, or both PTX and αFAP-PE38. Tumor sections were stained for CD31 (blood vessels) or F4/80 (macrophages). (*c*,*d*) Quantification of CD31-positive blood vessels and F4/80-positive macrophages in 4T1 tumors from the treated and untreated mice, as in (*b*). Data are representative of two independent experiments. (*: $p<0.05$).